Infrared Spectra of Carbonyl Hemoglobins: Characterization of Dynamic Heme Pocket Conformers†

William T. Potter,‡ Jo H. Hazzard,§ Miles G. Choc,⊥ Melvin P. Tucker,∥ and Winslow S. Caughey*
Department of Biochemistry, Colorado State University, Fort Collins, Colorado 80523
Received February 9, 1990; Revised Manuscript Received March 30, 1990

ABSTRACT: The infrared spectra for carbon monoxide complexed to hemoglobins were examined in the C–O stretch region. Deconvolution of the spectra requires four bands and supports the presence of four distinct conformers at the ligand binding site. Most typical hemoglobins exhibit only one predominant conformer for each subunit represented by a band at 1951 cm^{-1} in contrast to myoglobins, which typically exist in two major conformations. Several hemoglobins with an enlarged heme pocket are shown to shift the C–O frequency into the higher frequency conformer regions. Many factors, including pH, temperature, solvents, and divalent metals, are also shown to be capable of expanding the heme pocket. Only very specific structural changes that can reduce the size of the heme pocket will result in the lower frequency conformers. The weighted averages of the multiple CO vibrational frequencies are linearly related to the single ^{13}CO NMR chemical shift values and to the exponential of fast CO on-rates. Conformer interconversion occurs at a rate greater than 10^4 s^{-1}. The infrared C–O stretch spectra provide qualitative and quantitative information on the structural dynamics, stability, and ligand binding properties of hemoglobins.

Oxygen binding to hemoglobin can only occur with some flexibility in protein structure (Fermi et al., 1984). The protein dynamics involve an opening of the heme pocket for ligand entry and many more concerted motions that modify the heme's affinity for the ligand and the stability of the complex. The overall protein motions are complex and a detailed understanding requires a precise, quantitative description of the ligand–heme binding site. Vibrational spectroscopy of heme-bound ligands has been extremely useful in providing quantitative information on the liganded heme site environment (Caughey, 1980). In this paper the infrared C–O stretch bands are presented for a variety of carbonyl hemoglobins. The carbonyl ligand has well-characterized spectroscopic properties and its capacity for forming a stable complex makes it the most convenient reporter group for the heme site environment.

Each C–O stretch band reflects both the nature of the Fe–C bond and the interactions (steric and electrostatic) that occur between CO and its protein environments within the heme pocket. For MbCO, the structurally related monomeric protein, four carbonyl stretch bands have been observed in deconvoluted spectra (Caughey et al., 1981; Shimada & Caughey, 1982). The relative intensities of these four C–O stretch bands vary with pH, temperature, and solvent composition and support the presence of four rapidly interconverting structural conformers at the heme site. Similarly, multiple IR C–O stretch bands are observed in carbonyl Hbs (Caughey et al., 1978; Choc et al., 1981; Potter et al., 1983; Brown et al., 1983; Satterlee et al., 1978); however, the spectral analysis by deconvolution is less straightforward since bands for α and β subunits are overlapping in the $\alpha_2\beta_2$ tetramer. In the case of normal human HbA, each separated subunit has been shown to exhibit multiple C–O stretch bands (Potter et al., 1983). In this paper the respective contributions from each subunit to the total tetrameric spectrum are estimated. The weighted-average frequency of the multiple IR C–O stretch bands for each subunit are observed to be linearly correlated with the single ^{13}CO NMR chemical shift value. Similar, discrete, rapidly interconverting conformers exist in a wide variety of HbCO's. These Hb conformers appear structurally similar to those observed in the MbCO's. The functional implications of these structures are considered in regard to amino acid sequence differences. A minor conformer present in all Hb or Mb species appears to involve a transient enlargement or opening of the heme pocket of significance to ligand binding and stability properties.

Materials and Methods

Human and animal Hb hemolysates were prepared by hypotonic lysis of washed red cells (Riggs, 1981). Cellular debris was removed by centrifugation followed by extensive dialysis. This crude Hb preparation could be used directly or further purified. In certain cases Hb was stripped of organic phosphates by Dowex mixed-bed ion-exchange chromatography (Jelkman & Bauer, 1976). Further purification of Hb used DEAE ion-exchange chromatography. The Hb was converted to the carbonyl complex by extended exposure to CO gas without bubbling. Each HbCO was monitored by visible spectroscopy to determine complete CO saturation and assure the absence of metHb. Standard buffer was 0.1 M phosphate, pH 7.4. Changes in buffer composition or pH were accomplished by repeated dialysis against the appropriate CO saturated buffer. *N*-Ethylmaleimide Hb was prepared by incubating HbCO solutions with a slight excess of NEM at 4 °C for 12 h. Unreacted NEM was then removed by gel filtration.

Infrared spectra were recorded on a computer-interfaced Perkin-Elmer Model 180 or 580 double-beam spectrophotometer calibrated to within 0.1 cm^{-1} by using water vapor bands and set to 2.2-cm^{-1} resolution at 1950 cm^{-1}. Typical HbCO concentrations were 5–10 mM in heme. Constant-temperature cells with CaF_2 windows and ~0.05-mm path lengths were used. Matched reference cells with either HbO_2 or H_2O were required for flat base lines. Multiple scans (8–16) from 2000 to 1900 cm^{-1} were accumulated and averaged.

† Supported by U.S. Public Health Service Grant HL-15980.
‡ Department of Chemistry, University of Tulsa, Tulsa, OK 74104.
§ Department of Biochemistry, University of Arizona, Tucson, AZ 85712.
⊥ Sandoz Pharmaceutical, East Hanover, NJ 07936.
∥ SERI, 1617 Cole Boulevard, Golden, CO 80401.

0006-2960/90/0429-6283$02.50/0 © 1990 American Chemical Society

Spectra were analyzed by a curve-fitting procedure that used a linear combination of Lorentzian and Gaussian functions (Fraser & Suzuki, 1969). The same band shape (typically 30% Lorentzian and 70% Gaussian) was used for every band in a given spectrum. Changes to 100% Gaussian bands resulted in only minor variations in the band parameters but did slightly decrease the linearity of the residual between the observed and computed spectral bands. Other details of spectral measurements can be found in previous publications (Caughey, 1980; Caughey et al., 1981). Apparent integrated intensities (B, mM^{-1} cm^{-2}) were obtained from the total heme concentration as determined from the visibile spectrum of the CO complex (for human HbACO $\epsilon_{568.5}$ = 14.95 mM^{-1} cm^{-1}; Antonini & Brunori, 1971) and either the integration of the absorbance versus frequency spectrum or calculation of the area under the theoretical curves determined by deconvolution. The visible spectrum extinction coefficients for human HbACO were also used for the various animal HbCO's.

^{13}C NMR spectra on ^{13}CO-substituted samples were recorded at the Colorado State University Regional NMR Center on a JEOL FXN-100 NMR spectrometer operating at 25.1 MHz and 20 °C as described previously (Caughey et al., 1981). The ^{13}C resonance at 184.5 ppm from TMS for unbound ^{13}CO was used as an internal standard.

Results

Detection of Multiple C–O Stretch Bands in Hemoglobin Carbonyls. The quantitative analysis of IR HbCO spectra by deconvolution is illustrated in Figure 1. The major C–O vibrational envelope of a human HbACO spectrum is only partially fitted by a single symmetric curve located at 1951.2 cm^{-1}. The residual that results from subtraction of the single computed curve from the measured spectrum still exhibits an absorbance at 1969 cm^{-1} and a broad asymmetric absorbance extending from ~1945 cm^{-1} to lower wavenumbers. These other absorbance regions require three symmetric curves at 1969, 1943, and 1932 cm^{-1} to adequately approximate the observed HbACO spectrum (Table I). These four bands are labeled I–IV according to increasing wavenumber. Although bands I, II, and IV combined account for only ~5% of the total integrated intensity of the C–O vibrational envelope for human HbACO under physiological conditions of pH and temperature as in the red cell in vivo, absorbances in these regions are consistently observed. Furthermore, as we present here, under certain conditions, or in certain other Hb species, one or more of these three bands can be particularly prominant. Nevertheless, most vertebrate HbCO's from mammalian (Figure 2), avian, reptilian, and piscine species that we have investigated (Caughey et al., 1978) exhibit only one major band near 1951 cm^{-1} and only limited absorbance intensity is found in the other regions. In all species the HbCO stretch bands are narrow, with half-band widths less than 10 cm^{-1}. The conservation of these spectral similarities among such a wide variety of species must reflect certain essential properties that are required for the binding of the physiological ligand, dioxygen, to the hemoglobins.

The major vibrational band near 1951 cm^{-1} contains overlapping contributions from both the α and β subunits of the tetrameric HbCO. The IR C–O stretch bands for the separated subunits of human HbACO have been observed to differ by only 1.1 cm^{-1} (with the α-subunit band absorbing at the lower wavenumber) (Potter et al., 1983). Both subunits have some absorbance in the band IV (1969 cm^{-1}) region; however, the lower wavenumber regions primarily result from the α subunits. The summation of the spectra for the separated HbA subunits resulted in a spectrum that was indistinguishable from the native tetrameric HbCO spectrum.

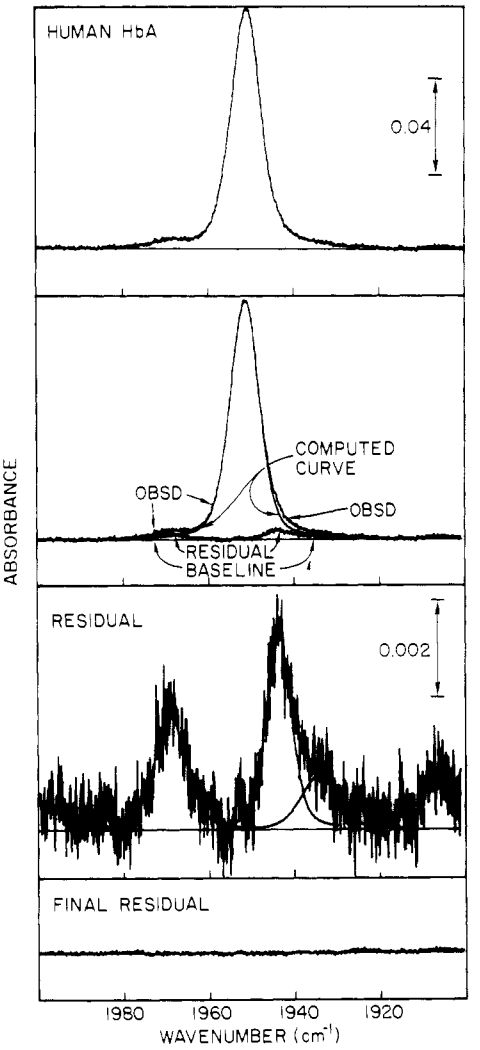

FIGURE 1: Deconvolution of the infrared spectrum of CO bound to human HbA. Top: Recorded spectrum for purified HbACO (5.5 mM in heme), pH 7.4, 30 °C. Middle: Deconvolution of the major absorbance with a single curve results in the residual difference between the symmetric, theoretical curve and the observed spectrum. Bottom: The residual is shown with an expanded absorbance axis. Deconvolution of the bottom panel requires three symmetric, theoretical curves. The final residual (shown without an expanded absorbance) results from subtraction of the sum of the four theoretical curves from the observed spectrum. The band parameters are listed in Table I. The low-intensity band near 1910 cm^{-1} is due to natural-abundance ^{13}CO bound to heme.

Hbs with Enhanced Minor Bands. The similarity between CO IR spectra for α and β subunits, discussed above for the typical Hbs, is not true for several Hb species in which a typically minor vibrational band is enhanced. It is significant that the Hbs with atypical CO IR spectra appear to exhibit unusual dioxygen binding and stability properties.

An example of enhanced band I is found among domesticated rabbits. Hb isolated from wild jackrabbits or cottontails displays a typical carbonyl spectrum with the predominant intensity at band III near 1951 cm^{-1} (Figure 3). However, the spectrum for each individual among the more than 20 different breeds of domesticated rabbits examined had an unusually intense band I. Hb isolated from New Zealand white rabbits (*Oryctolagus cuniculus*) exhibits two distinct types of carbonyl spectra. Both Hb types show elevated intensity in the band I region (Figure 3, Table I). The more common type (roughly 80% of the sampled population) contains 18–20% of the total absorbance in the band I region at

Table I: Parameters for Deconvoluted Infrared C–O Stretch Bands of Hemoglobin[a]

protein	temp (°C)	pH	band I ν_{CO} ($\Delta\nu_{1/2}$) (cm^{-1})	band I % A	band II ν_{CO} ($\Delta\nu_{1/2}$) (cm^{-1})	band II % A	band III ν_{CO} ($\Delta\nu_{1/2}$) (cm^{-1})	band III % A	band IV ν_{CO} ($\Delta\nu_{1/2}$) (cm^{-1})	band IV % A
Parameters of Hemoglobin Tetramers										
human HbA	28	7.4	1932 (8)	0.8	1943 (10.5)	4.4	1951.1 (8.1)	93.0	1969.5 (7.5)	1.8
	4	7.4			1943 (10.5)	3.2	1950.9 (7.8)	96.0	1969.5 (7.5)	.8
	30	5.0	1930 (10)	1.1	1043 (8)	2.7	1051.5 (7.9)	87.6	1968.5 (9)	8.6
	30	9.5	1930 (10)	1.4	1942.5 (8.5)	2.9	1951.0 (8.0)	94.1	1969.0 (9)	1.6
horse Hb	30	7	1931.5 (8)	0.9	1942 (8)	3.7	1949.7 (8.1)	94.2	1968 (7)	1.1
	9	7	1930 (8)	1.0	1941.5 (7.5)	3.3	1949.3 (7.8)	95.0	1969 (7)	0.7
cow Hb	36	7	1932 (8)	0.9	1941 (8)	2.7	1950.0 (8.4)	94.1	1968 (8.9)	2.3
	7	7	1931.5 (8)	0.6	1940.5 (7)	1.4	1949.6 (8.1)	96.3	1968 (8)	1.7
cottontail rabbit Hb	30	7	1935 (10)	1.7	1943.5 (8)	5.1	1950.6 (8.2)	90.2	1968 (8)	3.0
	10	7	1935 (10)	1.6	1944 (8)	3.4	1950.3 (8.1)	93.0	1970 (8)	2.0
opossum Hb	28	7	1930 (12)	1.3	1943 (9.35)	33.3	1948.4 (7.5)	14.3	1968.5 (12)	3.2
							1950.4 (10)	47.9		
	4	7	1930 (12)	1.3	1943 (9.4)	34.1	1948.4 (7.5)	14.2	1968 (12)	2.5
							1950.4 (10)	47.9		
white rabbit I Hb	29	7	1929.1 (10.5)	20.1	1946.8 (11)	7.4	1951.8 (7.9)	70.2	1970 (8)	2.3
	5	7	1928.7 (10.2)	20.6	1944 (10)	1.9	1951.2 (7.8)	75.6	1971 (8)	1.9
	29	5	1930.4 (10)	16.8	1945 (9)	3.2	1951.2 (7.9)	68	1968 (10)	12.0
	8	5	1929.8 (10.5)	18.3			1951.5 (7.8)	68.5	1968.5 (10)	10.1
white rabbit II Hb	29	7	1928.9 (10)	35.5			1951.8 (7.9)	62.0	1970 (9)	2.5
	4	7	1928.4 (10.2)	38.9			1951.2 (7.5)	59.0	1969 (9)	2.1
guinea pig Hb 30	30	7	1930 (7)	2.7	1941.5 (8.5)	5.2	1949.2 (9.6)	82.0	1965.6 (8.2)	10.0
	8	7	1930 (6.5)	1.8	1941.5 (8)	5.2	1948.75 (9.0)	85.0	1965.6 (8.0)	8.0
rat Hb	31	7	1933 (9)	3.2	1943 (10)	7.4	1950.3 (8.9)	75.5	1966.8 (7.5)	13.9
	4	7	1931 (9)	1.9	1941 (10)	6.6	1949.6 (8.5)	81.0	1966.8 (7.2)	10.5
mouse Hb	28	7	1933 (10)	2.5	1943 (10)	2.4	1950.8 (8.6)	85.8	1967.5 (11.5)	9.3
	5	7	1931 (10)	1.2	1941.5 (10)	3.5	1950.3 (8.2)	89.0	1967.5 (11.5)	6.3
carp Hb[b]	25	6.3			1945 (8)	6.9	1951.2 (8.5)	87.4	1967 (9)	5.7
carp Hb + IHP[b]	25	6.0			1946 (7)	4.9	1951.7 (9)	70.0	1969 (12)	25.1
human HbA + Zn^{+2} (gel)	28	6.6			1944 (9)	1.8	1951.3 (7.7)	71.5	1964 (10)	26.7
	4	6.6			1946 (9)	2.1	1951.1 (7.4)	77.2	1964 (10)	20.7
human HbA + NEM in 0.10 M phosphate	28	6.0			1943 (10)	5.1	1951.0 (7.7)	89.8	1969 (10)	5.1
+ Zn^{+2} (gel)	28	6.6			1945 (10)	4.95	1950.7 (8.2)	85.7	1967 (9)	9.8
bovine Mb[c]	35	7.8	1938 (18.5)	51.3	1943.5 (9.0)	42.8	1953.5 (9.0)	2.9	1965 (10)	3.0
	8	7.8	1938 (17)	45.4	1943.4 (8.4)	51.1	1953.6 (8.0)	2.5	1965 (10)	1.0
	20	5.2	1939 (17)	37.6	1945.5 (9.3)	46.5	1953.0 (9.0)	4.5	1965 (10)	11.4
sperm whale Mb	20	7.8	1933.4 (13.6)	39.6	1944.0 (8.7)	50.7	1952.0 (9.5)	7.2	1966 (10)	2.5

protein		band I ν_{CO} (cm^{-1})	band I % A	band II ν_{CO} (cm^{-1})	band II % A	band II ν_{CO} (cm^{-1})	band II % A	band IV ν_{CO} (cm^{-1})	band IV % A
Parameters of Hemoglobin Subunits									
human Hb[d]	α	1934	1.3	1943.5	3.3	1950.4	44	1969	1.2
	β					1951.9	49	1969	1.2
HbZurich[e]	α	1933.5	1.3	1943	3.3	1950.0	44	1969.1	1.2
	β	1933.5	0.4	1943	3.8	1958.2	40	1969.1	6.1
HgSydney[f]	α	1937	1.3	1944.1	3.3	1951.7	44.15	1967.7	1.2
	β	1937	1.0	1944.1	3.8	1951.7	28.05	1967.7	2.8
						1955.9	14.3		
rabbit HbI[e]	α_{Ab}	1929.1	20	1946.8	0	1950.9	4.33	1970	0.6
	α_{NOR}	1929.1	0	1946.8	7.4	1950.9	17.02	1970	0.6
	β	1929.1	0	1946.8	0	1952.4	48.9	1970	1.1
rabbit HbII	α	1928.9	36			1950.9	13	1970	1.2
	β	1928.9	0			1952.4	49	1970	1.2

[a] The area of each band was calculated as area = (maximum absorbance)($\Delta\nu_{1/2}$)(f) = 1.571 for a Lorentzian distribution and f = 1.065 for a Gaussian distribution (Fraser and Suzuki, 1969). For Hb spectra, a linear combination of these two functions in the range of 70% Gaussian gave the best fit. For Mb spectra, 100% Gaussian bands gave the best fit. [b] Onwubiko et al., 1982. [c] Shimada & Caughey, 1982. [d] Potter et al., 1983. [e] Potter et al., 1985. [f] Caughey et al., 1978. HbSydney presented here is a 30% mixture with HbA.

1929 cm^{-1}. The less common type exhibits nearly double this intensity at the same wavenumber. From the correlation of IR carbonyl spectra with ^{13}C NMR spectra (vide infra), we conclude the enhancement of the band I intensity is due to an altered α subunit. The variation among the rabbits appears to result from the presence of either one or two altered α subunits in the tetrameric Hb.

Opossum HbCO (*Didelphis marsupialis*) is a species whose Hb carbonyl spectrum exhibits enhanced band II intensity at 1943 cm^{-1} (Figure 4, Table I). This increase in band II intensity is clearly evident upon considering the deconvoluted spectrum. Again, the increase in the band II intensity is attributed to the α subunit of opossum Hb (vide infra). The α subunit of opossum Hb contains two substitutions of residues at the heme site that are normally in contact with the bound carbonyl ligand (distal E-7 His to Gln and distal E-11 Val to Ile; Stenzel et al., 1979).

Two human Hbs with substitutions at these same positions, but in the β subunits, have also been observed to alter the carbonyl stretch bands (Choc & Caughey, 1981; Tucker et al., 1978; Potter et al., 1985). In human HbZurich CO the distal E-7 His to Arg substitution shifts approximately 40% of the major vibrational band from 1951 cm^{-1} to 1958 cm^{-1} and intensifies band IV. However, band IV is observed at the same wavenumber as for normal HbACO (Table I).

In a similar manner, the distal E-11 Val to Ala substitution

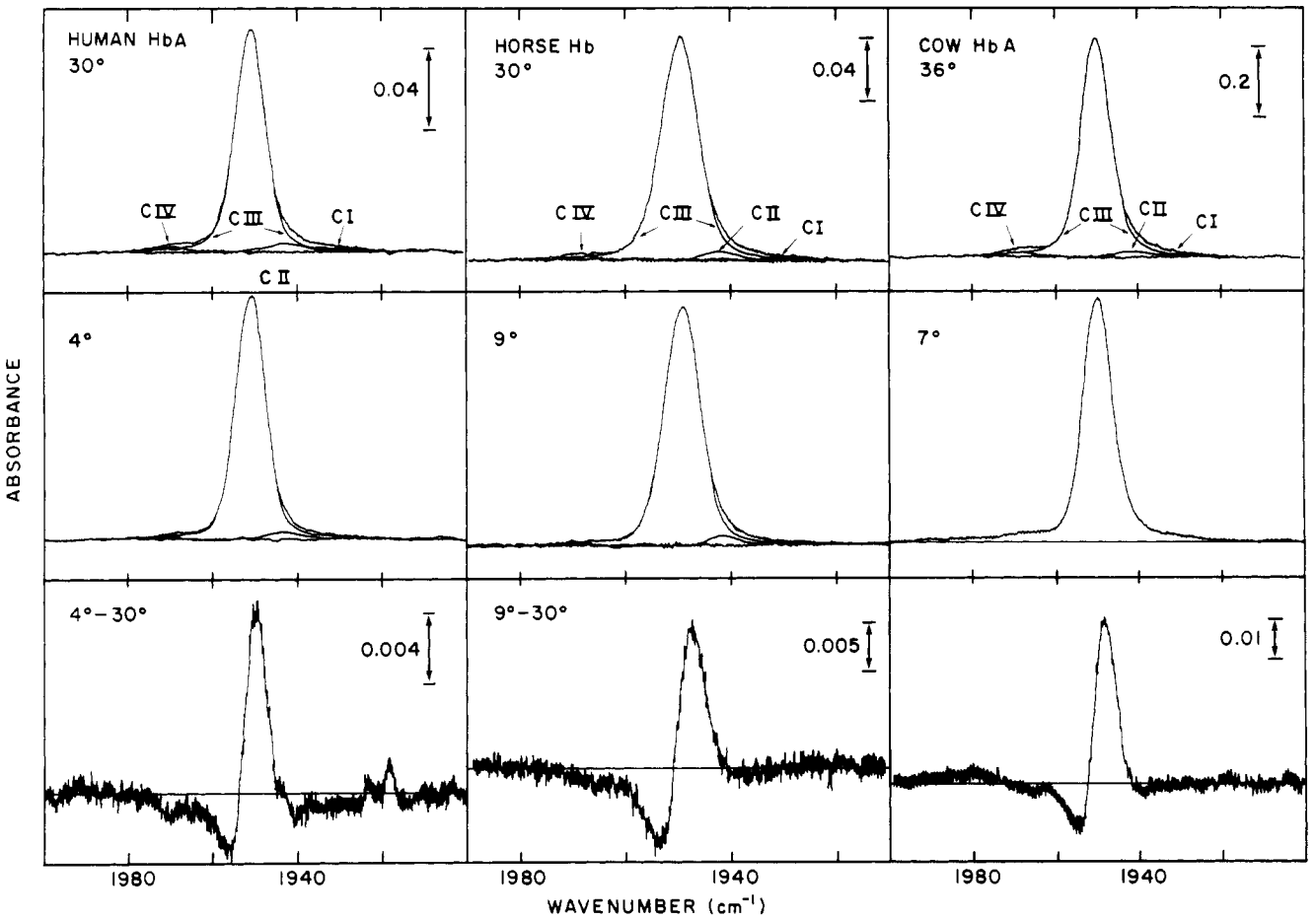

FIGURE 2: "Typical wild-type" HbCO IR CO spectra. Human, horse, and cow HbCO are shown at higher temperature in the top panel and at lower temperature in the middle panel. The temperature difference spectrum (low minus high temperature) is shown in the bottom panel with an expanded absorbance. The four bands of deconvolution are labeled CI–CIV in order of increasing wavenumber ("C" denotes IR CO stretch band *conformer*). Band parameters (band frequency, half-band width, and absorption maximum) are listed in Table I.

in human HbSydney β subunits shifts some of its band III intensity to $\sim$1955 cm^{-1} and increases the band IV intensity (Table I). Major shifts in wavenumber occur only for the predominant band III in either HbZurich or HbSydney and only minor frequency differences occur for the band IV position. This strongly suggests that band IV is a structural conformer with minimal interaction between these two important distal residues. Although both of these altered Hbs show increased intensity of band IV, band III must still be considered their major conformer.

There are certain species, e.g., rodents, with Hbs which appear to have slightly elevated amounts ($\sim$10%) of this highest frequency band (band IV), even though their major conformer is still observed near $\sim$1950 cm^{-1}, a typical band III position (Figure 5).

In spectra observed near pH 7 and <40 °C the half-band widths of all bands are relatively narrow (<10 cm^{-1}) (Table I).

Temperature-Induced Changes in HbCO Stretch Bands. Higher temperatures increase the band IV intensity near 1969 cm^{-1}. The "typical" wild-type HbCO spectrum shows substantial intensification of band IV when the temperature is increased from 4 to 30 °C (Figure 2, Table I). Higher temperatures also slightly broaden and shift band III.

The opossum and white rabbit HbCO spectra (Figure 4) exhibit the same general shift from lower to higher wavenumber bands when the temperature is elevated. Without exception, higher temperatures enhance the relative amounts of the higher wavenumber bands, but the extent of redistribution depends on the specific Hb species.

The temperature-dependent denaturation of human HbF CO upon raising the temperature to 80 °C is shown in Figure 6. The first two curves (at $\sim$20-min intervals) occur before complete temperature equilibration ($\sim$50 and 65 °C, respectively, as measured from cell window temperatures). Some band broadening is evident in the band IV region at intermediate temperatures. The half-band width of band IV increases steadily from 9 cm^{-1} at physiological temperatures to $\sim$30 cm^{-1} in the fully thermally denatured state.

The increase in half-band width is expected as the protein structure is denatured. The intimate environment surrounding the bound carbon monoxide becomes less ordered (as observed by band broadening). It is interesting to note how tenaciously the environment that gives rise to band III remains intact even after prolonged periods at an elevated temperature. Furthermore, the band III half-band widths are only slightly altered as band intensity decreases (particularly when compared to band IV).

Other Factors That Increase Band IV. The C–O stretch bands are sensitive to changes in pH (Choc & Caughey, 1981). Exposure of human HbACO to unphysiological pH increases band IV intensity (Figure 7). However, there is a range between pH 5.5 and 10 over which band IV intensity varies only slightly. Outside of these regions band IV intensity increases dramatically. Between pH 4 and 12 the spectral changes can be reversed by reincubation to physiological pH. The half-band widths for band IV increase by only 1–2 cm^{-1} at the extremes of pH.

The above changes in pH were accomplished slowly by extensive dialysis. A pH shock achieved by the direct addition

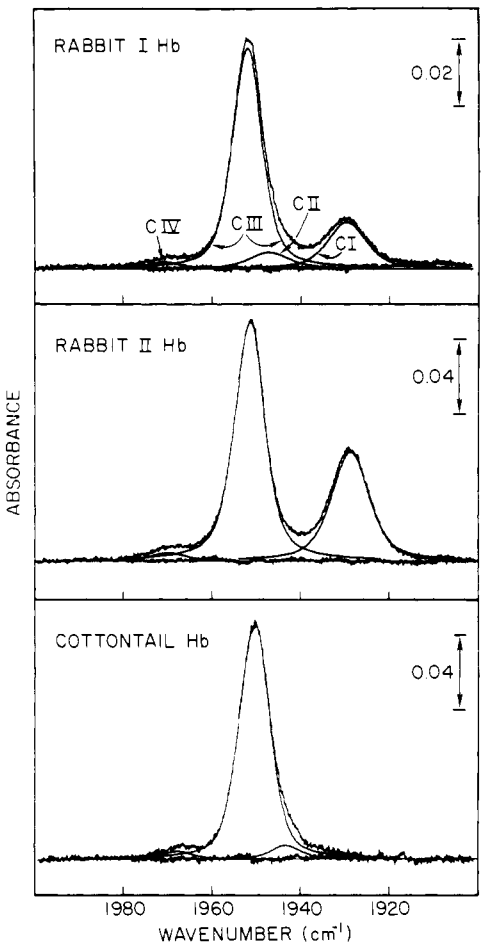

FIGURE 3: IR CO spectra for three distinct types of rabbit HbCO. Spectra for two types of domesticated rabbit (New Zealand white) HbCO with enhanced band CI intensity appear in the top and middle panels. The spectrum of cottontail HbCO (shown in the bottom panel) is of the "typical wild type". Band parameters are listed in Table I.

of 2 N HCl causes extensive gellation of HbCO; however, the IR spectrum was not significantly modified (although reduced in total intensity). In a similar manner HbCO could be gelled or precipitated by addition of polyethylene glycol, urea, or NH_4SO_4 without significant increases in band IV (data not shown). Other specific denaturants, however, such as SDS, DMSO, or ethanol, do increase a broad band in the band IV region that is consistent with a general disruption in the protein structure at the heme site (Figure 8). The time-dependent denaturation of HbCO is shown in Figure 9. The human HbCO sample in 70% ethanol could be stored at 4 °C with only minor spectral changes; however, upon warming the sample to 35 °C, the spectrum showed denaturation at the heme site within 30 min with the appearance of a broad band in the band IV region at 1967 cm^{-1}.

Divalent heavy metals, such as Zn^{2+}, Pb^{2+}, Ni^{2+}, or Pd^{2+}, will also gel HbACO. $ZnSO_4$, at Zn/heme ratios of 0.5, gels HbACO and shows a marked increase in intensity in the band IV region at 1964 cm^{-1} (Figure 10, Table I). This frequency is shifted from the usual band IV position at 1970–1969 cm^{-1} observed for the temperature or pH perturbations. Dialysis of the gelled HbCO solution against EDTA completely reverses both the gellation and IR effects. The addition of excess $PbCl_2$, $NiCl_2$, or $PdCl_2$ to HbACO solutions also increases band IV but at more typical wavenumbers (1969, 1970.5, and 1968 cm^{-1}, respectively). The band IV half-band widths observed for HbCO's treated with these metals were all less than 10 cm^{-1}.

Table II: ^{13}CO Resonances and Weighted-Average ^{12}CO Frequencies[a] for Hb, Mb, and Heme Carbonyls[b]

sample	δ (ppm)	$\bar{\nu}_{CO}$ (cm^{-1})
HbZh, β subunit, pH 7.7	205.5[c]	1957.8[c]
HbA, β subunit, pH 4.55	205.7[c]	1955.8[c]
jackrabbit Hb, β subunit	205.9	1952.8[d]
rabbit I Hb, β subunit	205.9	1952.9
rabbit II Hb, β subunit	205.9	1952.8
mouse Hb, β subunit	206.0[e]	1953.2
opossum Hb, β subunit	206.0	1950.9
carp Hb, β subunit, pH 6.0	206.0[f]	1952.7
rat Hb	206.0	1951.5
HbA, α subunit, pH 4.55	206.1[c]	1954.2[c]
β-chain from HbA, pH 7.2, 4 °C	206.1	1951.6
guinea pig Hb, β subunit	206.1[e]	1950.9
bovine Hb, β subunit, 36 °C	206.2[e]	1951.1
HbA, β subunit, pH 7.4	206.3[c]	1952.4
rabbit I Hb, α subunit	206.4	1950.2
carp Hb, α subunit, pH 6.0	206.5[f]	1950.6
jackrabbit Hb, α subunit	206.5	1950.8[d]
horse Hb, β subunit	206.5	1950.5
HbZh, α subunit, pH 7.7	206.5[c]	1949.6[c]
mouse Hb, α subunit	206.7[e]	1950.1
α-chain from HbA, pH 8.2, 4 °C	206.7	1950.2
bovine Hb, α-subunit, 36 °C	206.7[e]	1948.8
HbA, α subunit, pH 7.4	206.8[c]	1949.9
horse Hb, α subunit	206.8	1948.2
guinea pig Hb, α subunit	206.9[e]	1948.8
opossum Hb, α subunit	207.2	1944.6
bovine Mb, pH 8.4, 4 °C	207.7[g]	1941.4[g]
equine Mb	207.8[h]	1941.8[g]
sperm whale Mb	207.9[h]	1941.6[g]
rabbit II Hb, α subunit	207.9	1935.8
rabbit I Hb, α subunit	208.0	1933.8
N-butylimidazole heme B dimethyl ester in		
CCl_4, 4 °C	203.6[i]	1980[i]
$CHCl_3$, 4 °C	204.3[i]	1968[i]
Me_2SO, 4 °C	205.2[i]	1952.5[i]

[a] ν_{CO} values were calculated from the band locations and relative band intensities as indicated in the text. [b] Conditions of NMR and IR experiments are 30 °C and neutral pH unless listed otherwise. "Subunit" refers to the contribution of a particular α or β subunit to the tetramer spectrum. "Chain" is used when referring to spectra of separated subunits. [c] Choc & Caughey, 1981. [d] Choc (1979) Thesis, Colorado State University. [e] Moon & Richards, 1974. [f] Onwubiko et al., 1982. [g] Shimada & Caughey, 1982. [h] Moon et al. 1977. [i] Smith (1980) Thesis, Colorado State University.

Alkylation of the β-93 sulfhydryl of HbACO by NEM results in a slight red shift of the major band III frequency by ~1 cm^{-1} and a minor increase in band IV (Table I). This alkylation modifies the effects of Zn^{2+}. When a NEM-modified HbCO is treated with Zn^{2+}, the resultant gelled Hb solution increases band IV intensity by only ~1/2 of that observed with HbCO not treated with NEM. Furthermore, the band IV frequency occurs at 1967 cm^{-1} (as opposed to 1964 cm^{-1} for the unmodified HbCO) (Table I).

Other compounds that increase band IV intensity include acetylsalicylate, ascorbate, and glutathione, substances that can promote oxidation of oxygenated Hb (Wallace & Caughey, 1975; Sampath & Caughey, 1985). The half-band widths for band IV were all less than 10 cm^{-1} (data not shown).

^{13}C NMR Spectra of Carbonyl Hemoglobins. The "wild-type" HbCO's that exhibit a predominant band III near 1951 cm^{-1}, such as human HbACO, typically show two ^{13}CO resonances that differ by ~0.7 ppm, near 206.4–206.9 ppm for α subunits and 205.9–206.5 ppm for β-subunits (Table II). A larger range in ^{13}C resonances (2.5 ppm) is observed for HbCO species that show unusual C–O IR spectra. The β subunit of HbZhCO exhibits the lowest ^{13}C resonance at 205.5 ppm. The atypical rabbit HbCO exhibits the highest ^{13}C resonance at 208.0 ppm. The white rabbit individuals that

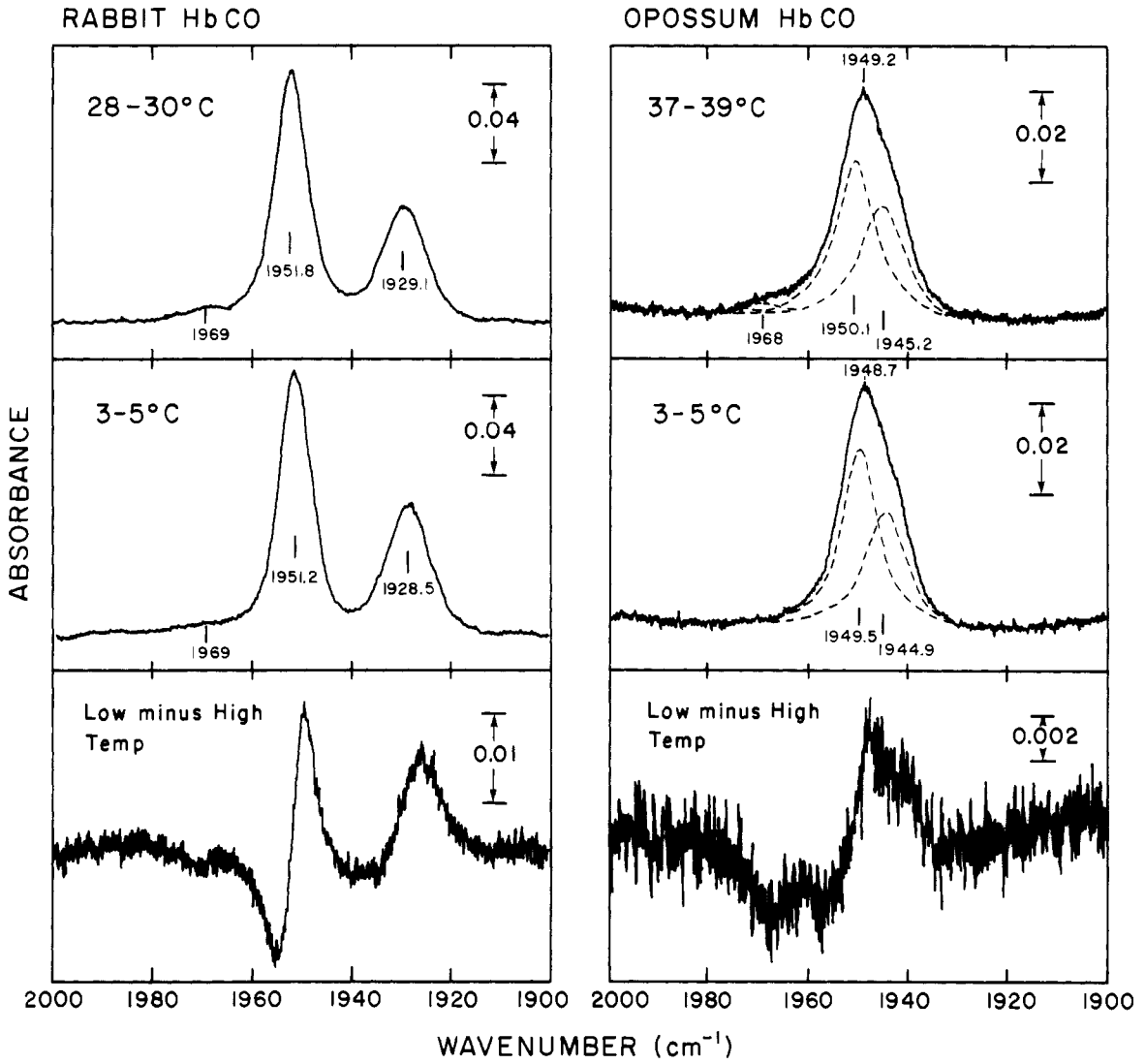

FIGURE 4: Temperature effects on IR CO spectra for HbCO species with enhanced lower wavenumber bands. Left: Rabbit HbCO (an enhanced band I species). Right: Opossum HbCO (an enhanced band II species). The bottom panels show the expanded low minus high temperature difference spectra for the respective HbCO's.

exhibit lower CO IR band I intensity show three ^{13}C NMR resonances—one ^{13}C resonance that is attributable to the β subunits (205.9) and two higher parts per million resonances, each with half the intensity of the β subunit. This observation supports the presence of both a normal and an abnormal α-subunit at 206.4 and 208.0 ppm, respectfully. The white rabbit individuals with greater CO IR band I intensities show only two ^{13}C NMR resonances of equal intensity, one at 205.9 ppm attributable to β subunits and one at 207.9 ppm for an abnormal α subunit. Two well-resolved ^{13}C NMR resonances are evident in opossum HbCO, which has an elevated band II CO IR. One resonance corresponds to a normal β subunit at 206.0 ppm and the other to an altered α subunit at 207.2 ppm.

Correlation of IR Carbonyl Stretch Frequency with ^{13}C NMR Chemical Shift. The carbonyl stretch frequency and the ^{13}C NMR chemical shift are both related to the CO bond order. A plot of weighted-average ν_{CO} versus δ is essentially linear (Figure 11). The use of weighted-average ν_{CO} is required since subunits exhibit absorbance at more than one frequency and yet have only one NMR resonance. For most wild-type HbCO's nearly all of the C–O stretch intensity occurs in one band (band III), and therefore, the weighted-average frequency occurs very near the band III frequency. For purposes of estimation of the weighted-average CO IR for each subunit, all Hb species with a predominance of one narrow band III can be assumed to have two bands of equal intensity in the band III region related to each subunit type. Using the observed differences for separated subunits of human HbA, band III can be deconvoluted with good approximation by using two bands separated by 1.5 cm^{-1}. The intensities for band I and II are assigned only to the α subunit. The band IV intensity is equally divided between α and β subunits. This method results in weighted-average C–O frequencies for β subunits between 1952 and 1951 cm^{-1} and for the α subunits between 1950 and 1949 cm^{-1} (Table II).

For the HbCO's with unusual CO IR spectra (i.e., significant absorbance at frequencies other than 1951 cm^{-1}), the determination of a weighted-average vibrational frequency for each subunit rests on the assumption that only one subunit is altered from a "typical" state. This supposition can be cross-examined for consistency with both amino acid sequence and NMR data. For HbZhCO, subtraction of intensity due to a normal α subunit gives a good approximation of the spectral contributions that come from the β subunits (Table I). For white rabbit HbCO, subtraction of intensity for a normal β subunit gives a reasonable approximation of the α subunit's contribution to the total spectrum. For the rabbit species that exhibits only two ^{13}C resonances, ~13% of the α subunit intensity has to occur in the band III region to have

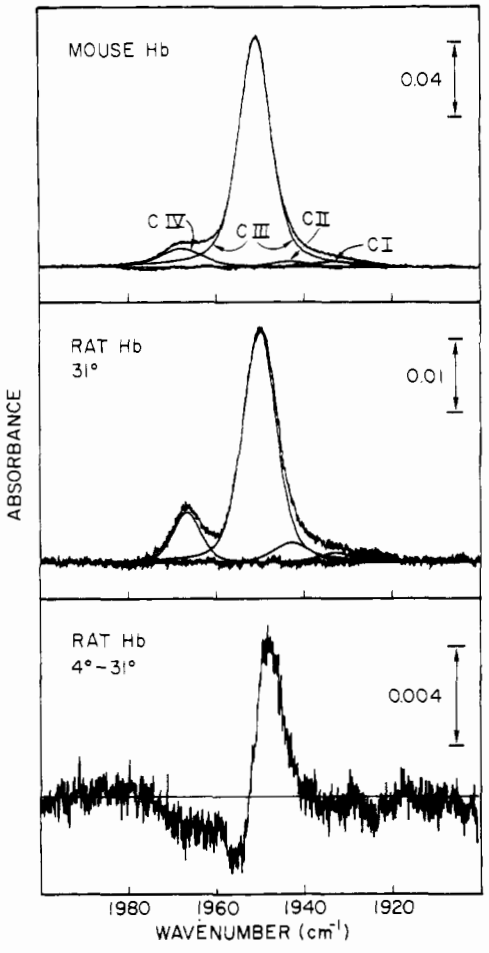

FIGURE 5: Representative IR CO spectra of rodent Hbs that show an enhanced band IV. Top panel: mouse HbCO at 28 °C. Middle panel: rat HbCO at 31 °C. Bottom panel: the rat HbCO temperature difference spectrum (4–31 °C).

equivalent contributions from both α and β subunits to the total spectrum. Similarly, opossum α subunits require ~14% of the total intensity in the band III region (Table I). The weighted-average vibrational frequencies are presented in Table II.

For the rodent HbCO's with elevated band IV it is uncertain which subunit contributes more to band IV. The rodent sequence data support the presence of many amino acid substitutions in both α and β subunits, and furthermore, the ^{13}C resonances for the separated subunits of these species have not been observed. The calculated distribution with equal subunit contributions to band IV is presented in Table II.

The correlation between the observed ^{13}C NMR resonances and the calculated weighted-average IR C–O frequencies is shown in Figure 11. Several HbCO species at different pHs and three different MbCO species are included in the linear correlation. This correlation does not extend to certain other species that do not contain a proximal histidine (e.g., cytochrome P-450). The ^{13}C resonances cover a 2.5 ppm range and the computed weighted-average vibrational frequencies vary by 24 cm^{-1}. This is nearly a 10-cm^{-1} change in ν_{CO} for each 1 ppm chemical shift.

Ligand Binding Studies. Both HbZh and white rabbit Hb show large differences in affinity for ligands between α and β subunits. Titration of the oxygenated species with CO shows a marked difference in CO affinity. For $HbZhO_2$, the β subunits, with the higher frequency bands, bind CO before the α subunits (Figure 12). For rabbits, which have the lowest frequency α subunit bands, a brief flush of rabbit carbonyl

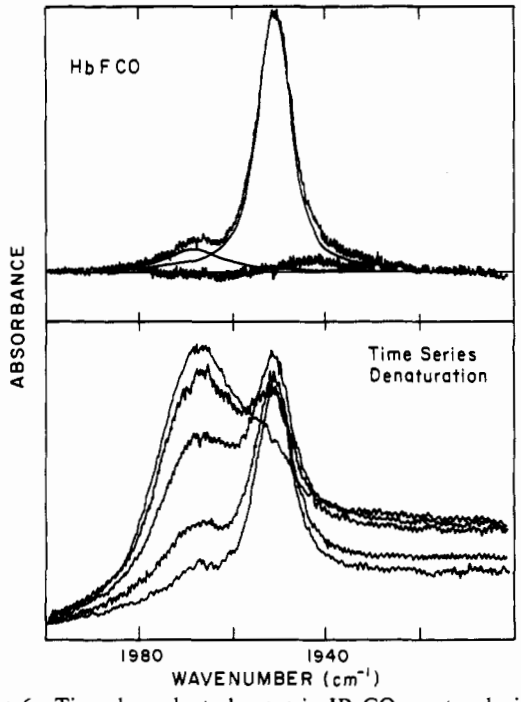

FIGURE 6: Time-dependent changes in IR CO spectra during the denaturation of HbF CO at elevated temperatures. Top panel: HbF CO at 35 °C (absorbance maximum approximately 0.1). Bottom panel: IR CO spectra observed with time of incubation at elevated temperatures. Curves 1, 2, and 3 (according to increasing absorbance at 1970 cm^{-1}) were observed at 20-min intervals and temperatures of ~50, 65, and 80 °C, respectively, as measured by IR cell window temperatures. The final two curves were observed after 2 and 3 h, respectively, at 80 °C. The changes in absorbance at 1920 cm^{-1} reflect an uncorrected base line; the nonlinearity of the base line is observed during denaturation.

Hb with O_2 results in the selective removal of CO from the α subunits. These results show that a general partitioning preference of CO over O_2 occurs with increasing C–O vibrational frequencies.

A plot of the weighted-average C–O frequencies against the log of the kinetic rate constants for CO binding is linear for several R-state Hb species (i.e., CO association rate for the fourth CO) (Figure 11). In many of the reported kinetic studies, however, both a fast and slow component is observed. No clear correlation appears applicable to the slow component or for the Hb's that are found in the T-state such a carp HbCO with IHP (Onwubiko et al., 1982). It should be noted that either Hb or Mb complexed with Zn^{2+} shows a general increase in CO affinity (Oelshlegel et al., 1973; Gilman & Brewer, 1978).

Heme Carbonyls. IR spectra of *N*-butylimidazole heme B dimethyl ester carbonyls exhibit broad bands and the frequency is sensitive to solvent parameters (Table II). As solvent polarity increases, lower C–O stretch bands are observed. The ^{13}C NMR resonances are linearly related to the C–O stretching frequencies; however, the slope is different than observed with the Hbs and Mbs and indicates that smaller changes in chemical shift occur in relationship to the IR stretch bands (Figure 11, Table II).

Discussion

HbCO IR Spectra. The C–O stretch band data for the HbCO's reported here significantly extend the data available for interpretation of these vibrational spectra. Four CO stretch bands were found between 1930 and 1970 cm^{-1} in regions generally similar to the regions where four bands were found in myoglobin carbonyls. However, the relative band intensities

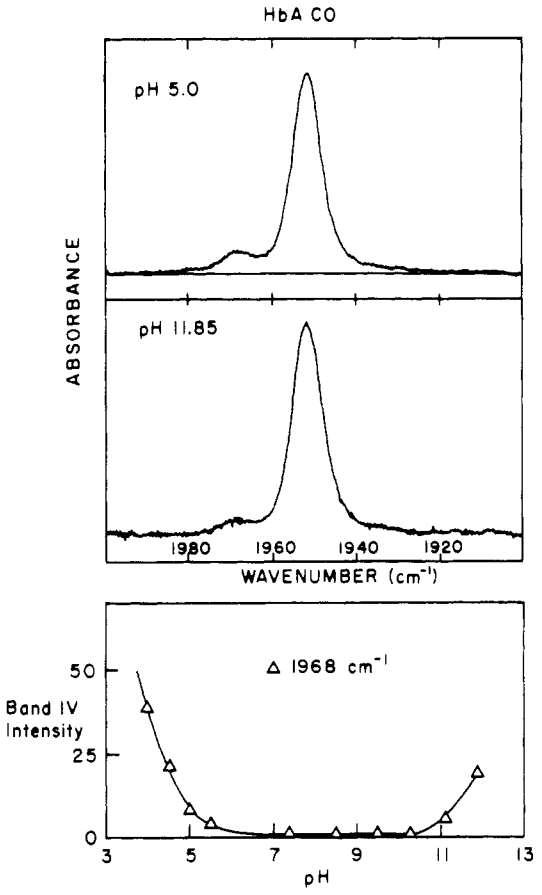

FIGURE 7: IR CO spectra of purified HbACO at high and low pHs. Top panel: HbACO at pH 5 (dialyzed versus 0.1 M citrate). Middle panel: HbACO at pH 11.85 (dialyzed versus 0.1 M borate). Bottom panel: Band CIV intensity versus pH for pH changes achieved slowly by dialysis (Choc & Caughey, 1981).

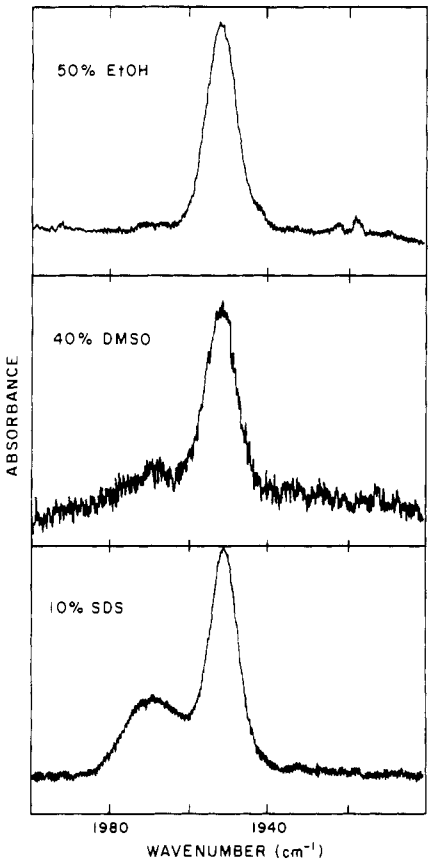

FIGURE 8: IR CO spectra of HbACO treated with solvents exhibit variable changes in band IV. IR CO spectrum of HbACO in 50% ethanol (top panel) exhibits very minor spectral changes from untreated Hbs. Spectra equivalent to this spectrum were also observed for HbCO precipitated with urea, NH_4SO_4, and HCl. Other solvents, such as 40% DMSO (middle panel) and 10% SDS, give rise to a broad band in the band IV region, indicating general ligand pocket denaturation. All spectra were observed at 25 °C in 0.1 M phosphate buffer with an absorbance maximum of approximately 0.05.

for HbCO's are characteristically different for Hb and Mb carbonyls. Typically, a HbCO subunit exhibits one strong band and three very weak bands. Variations in amino acid sequence can alter frequencies and/or intensities. For each of the four spectral regions, at least one HbCO has been found that exhibits a strong band. The spectra are particularly sensitive to changes in the amino acid residue at E-7 or E-11, the distal residues nearest to the CO ligand. Other factors that alter the spectra include temperature, pH, metal ions, and organic compounds. Denaturing conditions, e.g., high temperature or pH extremes, dramatically change the observed spectrum.

Utility of IR HbCO Spectra. These spectra provide unique information in relating protein structure to function. The techniques employed provide a convenient and useful method by which fundamental differences at the heme pocket of mutant Hbs and Hbs from different species under a variety of conditions, e.g., solution, crystal, amorphous precipitate, intact cells, or even a single red cell (Dong et al., 1988), can be characterized.

The spectra presented were analyzed by a deconvolution protocol that fits the spectrum with symmetrical bands. The observation of multiple stretch bands for the bound carbonyl can be obvious; however, determination of their parameters (ν_{CO}, $\Delta\nu_{1/2}$, and intensity) depends upon the method of spectral analysis. Deconvolution with symmetric bands is straightforward and supports the presence of four vibrational bands in each HbCO subunit. Other deconvolution procedures with asymmetric curves (using, for example, log normal distributions) may be used, but the theoretical basis for such deconvolution is not well formulated. The method of deconvolution presented here provides a basic framework for quantitative studies.

^{13}C NMR Spectra Support Rapid Interconversion among Conformers. Each C–O stretch band exhibited by a HbCO subunit can be attributed to a discrete protein conformer (Caughey et al., 1981; Shimada & Caughey, 1982; Potter et al., 1983). Although each subunit can have as many as four conformers, only one ^{13}C NMR resonance is observed. Only one NMR resonance for a subunit with multiple IR detectable conformers can be explained in terms of a rate of interconversion among conformers that is greater than the NMR time scale ($\sim 10^{-4}$ s). The linear correlation between weighted-average C–O stretch frequencies and NMR chemical shifts supports this explanation. The individual conformers cannot be measured directly by NMR spectroscopy because the NMR time scale is too long.

Conformer Structure. The evidence for multiple conformers that interconvert rapidly demonstrates the dynamic nature of the heme pocket. The wide differences in ν_{CO} for the four conformers in a given subunit are only consistent with substantial structural differences among the conformers. However, the band widths of 8–9 cm^{-1} reflect relatively little inhomogeneous broadening, which indicates that the conformer provides the CO ligand with an immediate environment that is relatively immobile.

The predominant conformer is expected to closely correspond to the X-ray structure if solution and crystal structures

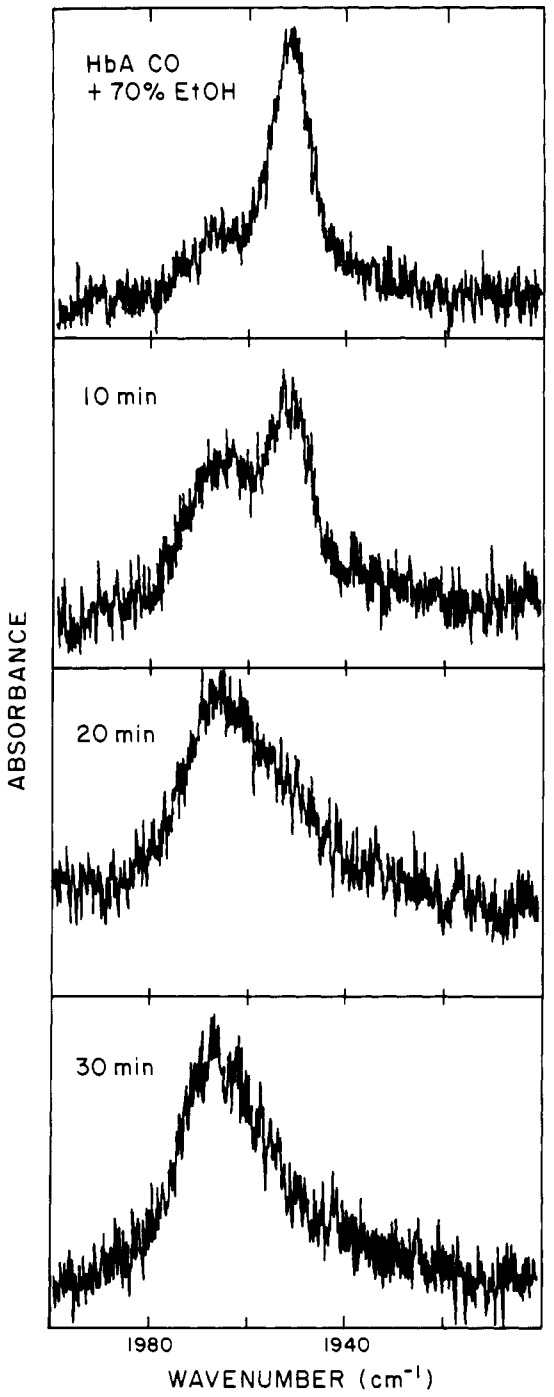

FIGURE 9: Time-dependent denaturation of HbACO with ethanol. IR CO spectra of HbACO in 70% ethanol at 35 °C, pH 7.4, over the time course of 30 min. The HbCO sample could be stored at 4 °C in ethanol without spectral changes but exhibited rapid denaturation upon warming to 35 °C.

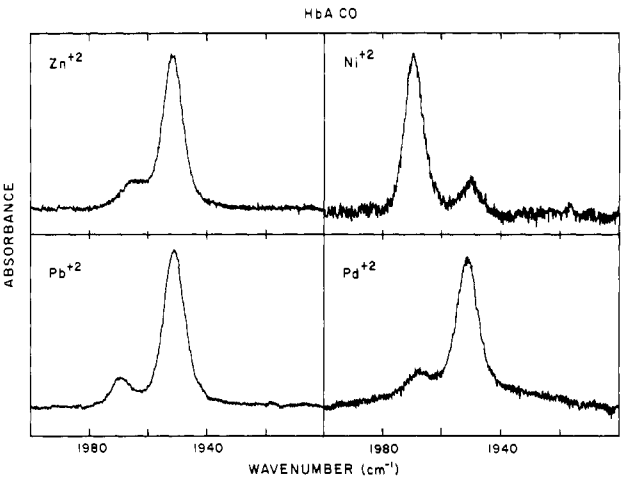

FIGURE 10: IR CO spectra of HbACO treated with divalent heavy metals. Top left: Zinc sulfate added to HbACO at a molar ratio of 0.5:1 gels the protein and increases a narrow band IV at 1964 cm^{-1}. Addition of excess lead, nickel, or palladium chloride to HbACO solutions also causes variable increases in a band IV near 1970 cm^{-1}.

are the same. The general similarity of solution and crystal structures is supported by IR spectra for HbACO and HbZhCO (Potter et al., 1985). However, with HbACO, band IV is somewhat enhanced and band III for β subunits is shifted to higher wavenumbers by 3 cm^{-1} in the crystal compared with solution. The spectra for HbZhCO in solution and crystal were nearly identical. In the HbACO X-ray crystallographic structure the carbonyl ligand is distorted from its preferred normal-to-the-heme-plane coordination (Heidner et al., 1976). The distal E-7 histidine and E-11 valine are in van der Waals contact with the ligand for the "typical" HbCO. The HbZhCO X-ray structure shows the distal Arg at E-7 of the β subunit shifted out of the heme pocket and attached to a heme propionic acid group (Tucker et al., 1978). For HbSydney, the distal E-11 substitution of Ala for Val leaves a void in the heme pocket. The X-ray structures are only applicable to the major conformer(s) since the minor conformers will contribute little to the "averaged" X-ray structure. In this regard it is of interest to note that the most recent X-ray crystal structure for MbCO (Kuriyan et al., 1986) has revealed the two conformers shown to be present earlier in solution and crystal CO IR studies (McCoy & Caughey, 1971; Makinen et al., 1979; Caughey et al., 1981).

Conformer Shifts: Enlargement of the Ligand Binding Pocket. A limited number of structural changes promote conversion of conformer III to conformer IV as shown by an intensity shift from band III to band IV. The reduction of steric interaction with CO at the distal E-7 and E-11 positions is reflected in spectra of HbZh (β E-7 His to Arg) and HbSydney (β E-11 Val to Ala); band IV is intensified and band III is shifted to the blue (Table I). Substitution at E-7 produces a larger shift than substitution at E-11. Site-directed mutation of E-7 His to Arg in bovine myoglobin results in a C–O stretch spectrum with major absorbance at 1957 cm^{-1} and generally similar to the HbZurich β-subunit spectrum (Shimada et al., 1989). Since the band IV frequency remains near the normal value for both HbZh and HbSydney, we conclude that the distal E-7 and distal E-11 interactions with bound CO in CIV are very weak and, possibly, nonexistent. However, Nagai et al. (1987), using human HbA mutants produced in *E. coli*, reported no changes in the C–O stretch in Raman spectra for the β E-11 Val to Ala substitution, the equivalent of HbSydney (weaker bands were not mentioned). The spectra were not deconvoluted; without deconvolution spectral shifts of 3–4 cm^{-1} may be overlooked. The validity of their conclusion, namely, that the β E-11 Val exhibits constraints only in the T-state, is therefore questionable.

The blue shifts in band III observed for HbZh and HbSydney may arise from decreased polarity of the ligand environment and/or a release of steric constraint on an orientation of CO normal to the heme plane. Model heme CO studies show that as solvent polarity is decreased, higher frequency C–O stretch bands are observed (Table II). Crystallographic studies show the packing constraints on the heme by the surrounding protein are tight (Deathrage et al., 1976). Ligands that prefer linear axial coordination (CO, CN^{-1}) expand the pocket more than ligands preferring bent

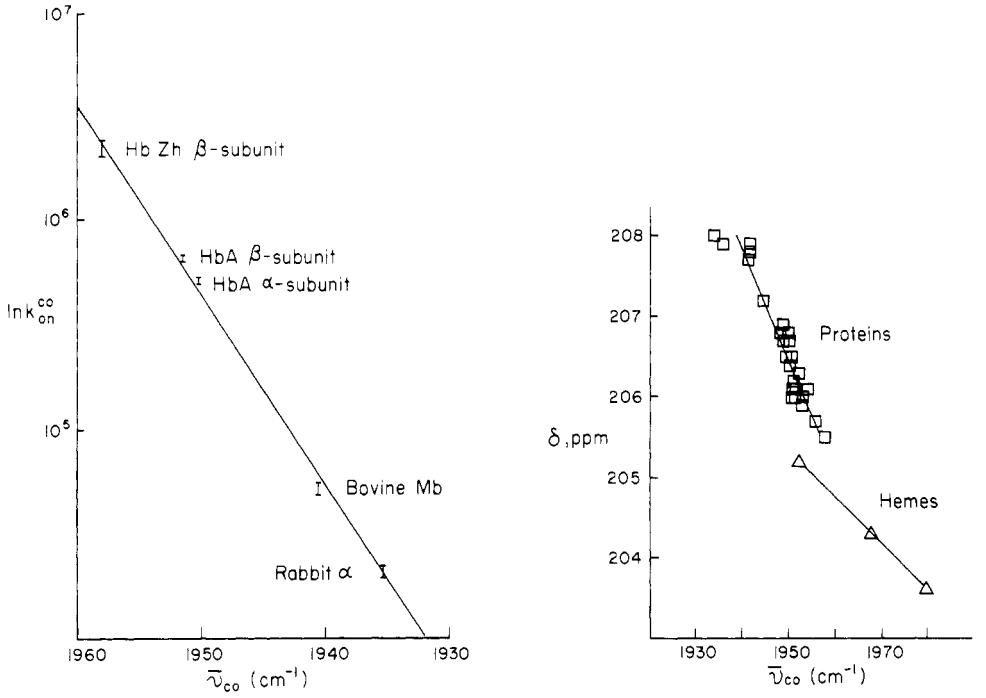

FIGURE 11: Correlations of weighted-average CO stretch frequency with the rate of CO binding and the ^{13}C NMR chemical shift. Right: Plot of ^{13}CO NMR chemical shifts in ppm versus weighted-average $\nu(^{12}CO)$ in cm^{-1} for the HbCO's and MbCO's. Data are tabulated in Table II. Left: Plot of ln K^{CO}_{on} versus weighted-average $\nu(^{12}CO)$ for HbZh β subunits, α and β subunits of human HbACO, bovine MbCO, and α subunits of white rabbit. Kinetic rates for rabbit α subunits and HbA taken from Sharma and Ranney (1982), for HbZh β subunits from Giacometti et al. (1980), and for bovine Mb from Antonini and Brunori (1971). In cases where both fast and slow rates are observed, only the fast rate is included.

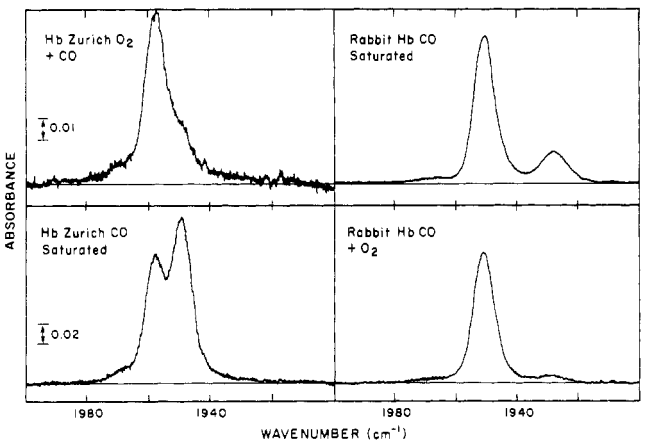

FIGURE 12: CO IR spectra of HbZurich and domesticated rabbit Hb in CO/O_2 mixtures. Left panels: IR CO spectra of $HbZhO_2$ briefly flushed with CO (top) corresponding to 40% total CO ligation primarily at the β subunits (Table I). HbZh completely saturated with CO (bottom). The β subunits of HbZh exhibit increased CO/O_2 partitioning preference. Right panels: IR CO spectrum of white rabbit (type I) packed red cells saturated with CO (top). IR CO spectrum of rabbit HbCO briefly flushed with O_2 (bottom). The rabbit α subunits exhibit a decreased CO/O_2 partitioning preference as exhibited by the decrease in band I intensity as O_2 replaces CO.

coordination (O_2, N_3^{-1}). Steric interactions by both the E-7 and E-11 residues interfere with linear binding and both CO and CN^{-1} are forced to bind off the heme normal axis. The strain generated by this interference is partitioned between bending of the ligand, deformation and tilting of the heme, and movement of the globin (Yoshikawa et al., 1985). For large ligands, the position of the distal histidine is so altered that it is actually rotated out of the heme pocket (Ringe et al., 1984). A basic question in protein dynamics is, to what extent do the protein dynamics correspond to local side chain rearrangements as opposed to overall concerted motions involving elements of secondary structure? It is well-known that large helical shifts occur upon ligation in both Hbs and Mbs (Liddington et al., 1988; Kuriyan et al., 1986). These shifts result in a ligand-dependent variation in the packing of the E and F helices at the heme. The CO stretch spectra for HbZh and HbSydney suggest that movements at the E-7 and E-11, at least, must occur to give rise to the band IV structure.

Several very specific sequences of low-energy protein motions at the heme pocket have been calculated for the formation of channels for ligand entry to or release from the heme pocket in sperm whale Mb (Case & Karplus, 1979). For one low-energy calculation, both the distal E-7 histidine and E-11 valine rearrange to open the channel. Band IV would be consistent with, but not necessarily restricted to, this type of concerted motion.

Band widths are found to increase as the mobility of the ligand environment increases. Band IV widths increase to $\Delta\nu_{1/2} > 30$ cm^{-1} with high-temperature denaturation; band IV is much narrower ($\Delta\nu_{1/2} < 10$ cm^{-1}) in native structures. A wide range of intensities and widths can be observed with highly insulted HbCO. These differences suggest different degrees of heme pocket enlargement and may result from either limited amino acid side chain motions or concerted rearrangements of secondary structure. The effects of medium on band IV were diverse. Precipitation with ammonium sulfate and urea showed only small increases in band IV that would correspond to only very minor structural changes occurring at the ligand binding pocket. Satterlee (1983) observed little effect of urea and guanidine chloride on ^{13}CO chemical shifts in ^{13}C NMR of hemoglobins. We find HCl-induced gellation has little effect on band IV. High concentrations of ethanol, DMSO, and SDS increased band IV with broadening suggestive of a random denaturation similar to that observed at the high temperatures.

Several reagents, including NEM, GSH, and divalent metals, that can react at the β-93 cysteine residue, show enhancement of band IV without broadening. The position of

the cysteine residue is considered a marker for T- and R-state Hb (Moh et al., 1987). In HbCO this residue is withdrawn into a nonpolar cavity following the motion of the adjacent proximal histidine at β-92. The combination of Zn^{2+} and NEM displayed a combined effect on both the intensity and position of band IV. These results suggest that although the IR-observable changes primarily reflect distal steric interactions, other less direct structural dynamics may also be involved in the shifts of the ligand vibrational bands.

A variety of metal ions, drugs, and other compounds promote the oxidation of Hb to metHb. Mechanisms involved include reaction of an electron acceptor with deoxyHb and the reaction of an electron donor with oxyHb (Caughey et al., 1982; Kawanishi & Caughey, 1985; Hegetschweiler et al., 1987). It is thus of interest that some compounds that promote metHb formation also increase band IV for the carbonyl Hbs.

In summary, band IV appears to reflect a reduction in the distal steric constraints on CO binding normal to the heme plane. Band IV may arise at one extreme from discrete side chain motions and at the other extreme from general shifts of secondary structure. The variations in widths and frequency observed for band IV indicate that a range of possible structures can form that differ in the degree of reduced distal interaction. The structural transitions that give rise to band IV may involve a continuum related to a general enlargement of the heme pocket. However, band IV of the native protein structure appears to be a well-defined structure.

Conformer Shifts: Contraction of the Ligand Binding Pocket. The alterations in protein structure discussed above have increased CO frequency. In no case did the pH, temperature, or solvent perturbations enhance the lower frequency bands. The heme appears very tightly packed within the overall helical packing constraints and very specific changes in protein structure are required to produce the lower frequency bands. The two HbCO species with enhanced lower wavenumber bands, opossum and white rabbit, have amino acid sequences consistent with a more restricted heme pocket. Opossum Hb with an E-11 isoleucine and E-7 glutamine (Stenzel et al., 1979), compared with HbA where E-11 is valine and E-7 histidine, is expected to place greater steric constraints on the CO ligand. Other factors such as the polarity difference between the side chains of glutamine and histidine may also play a role. For white rabbit Hb the presence of two allelic forms of the α subunit helps in the correlation of structural changes with IR bands. The two alleles contain residue differences at the B-10, CD-6, and CD-7 positions (Andersson et al., 1985). One allele corresponds to a normal B-10 Leu, CD-6 Leu, and CD-7 Ser sequence; whereas the abnormal allele contains B-10 Val, CD-6 Phe, and CD-7 Thr substitutions. Of these residues both the B-10 and CD-6 residues are certain to play some role in heme packing (Moon & Richards, 1974). Residue B-10 is in contact with the distal histidine and restricts its motion toward the heme perpendicular axis. The substitution of the smaller valine for leucine could allow the distal histidine to move even closer to the heme normal. The CD-6 substitution is not as obviously related to contraction of the heme pocket. The CD-6 residue forms the upper contact with the highly conserved CD-1, CD-3 phenylalanine network. This network forms the third major interaction with the distal heme pocket (besides the distal E-7 and E-11 residues). The substitution of CD-6 Val by Phe may therefore enhance the net CD corner interaction with the heme in the rabbit α subunit.

Two other lines of evidence support the interpretation of IR conformers in terms of structural changes involved in the size and extent of distal steric strain on the carbonyl ligand bound at the heme. First, the partitioning preference of CO versus O_2 observed for HbZh β subunits (Giacometti et al., 1980) and rabbit α subunits (Figure 12) strongly supports the role of distal restraints in binding the linear CO ligand. Second, the isotopic shift difference between $^{12}C^{18}O$ and $^{13}C^{16}O$ has been shown to increase with enhanced tilting/bending distortions of the CO (Yu et al., 1983; Carson et al., 1985). The abnormal rabbit α subunit band I shows the largest difference between the ^{12}C and ^{13}C isotopes (1.3 cm^{-1} for band I versus 0.1 cm^{-1} for band III).

Comparisons of CO Stretch Bands with Ligand Binding. In general, modifications (such as alkylation or reaction of Hb with Zn^{2+}) that increase CO affinity (Gilman & Brewer, 1978) also increase the amount of band IV conformer. However, direct correlations between either equilibrium or kinetic ligand binding parameters and the IR observed conformers are unclear. The fact that there appears to be some exponential correlation of rapid CO association rates and the average CO stretch frequency suggests that a determinant for carbon monoxide binding consists of an activation barrier related to distal steric interactions. Several low-temperature studies on MbCO have been able to freeze out conformer interconversion and to determine the distinct kinetic properties for each conformer (Chance et al., 1987; Alben et al., 1982; Alberding et al., 1978). The correlation of IR conformers to kinetic properties at physiological temperatures will undoubtedly be complex, involving both multiple barriers and multiple conformational states (Campbell et al., 1985).

Comparison of Hb and Mb Carbonyls. The CO IR spectra of both Hbs and Mbs show four bands for each protein chain. For HbCO there is a predominance of one band (band III) and disruption of the protein restraints increases the higher frequency conformer (band IV). Carbonyl Mbs exhibit two major bands (bands I and II), which shift to band IV at temperature or pH extremes. The band IV of Mbs is typically observed near 1965 cm^{-1}, 5 cm^{-1} less than observed for HbCO. A similar shift of 5 cm^{-1} was also observed between Hbs and Mbs for the two O–O stretch bands (Potter et al., 1987). O_2, a bent ligand, is subject to quite a different extent of distal steric interaction when compared to the CO (Moffat et al., 1979; Caughey, 1970). The difference between HbCO and MbCO is best correlated to enhanced distortion of the linear CO in MbCO compared with that of typical HbCO. For the already bent O_2 there appears to be an overall shift in the bound ligand's vibrational energy, which supports stronger Fe–O_2 bonding in Mb. In MbCO, band II at 1945 cm^{-1}, which contains ~50% of the total intensity, has a half-band width similar to the HbCO band III and would appear to correlate to the general 5-cm^{-1} shift observed for the CO band IV and the multiple O_2 bands. The band I of bovine MbCO (at 1938 cm^{-1}) is distinctly different with a large (18 cm^{-1}) half-band width.

Several types of linear correlations exist between the vibrational frequencies of heme bound CO and (1) the porphyrin pk_3 (Alben & Caughey, 1968), (2) the iron reduction potential (Smith et al. 1984), (3) the ^{13}C NMR resonances (this work; Satterlee, 1983), and (4) the O_2 binding affinity (Berzofsky et al., 1972). The fact that both CO and O_2 show similar shifts between Hbs and Mbs implies that direct steric differences between conformers for a 1950-cm^{-1} Hb carbonyl band and a 1945-cm^{-1} Mb carbonyl band may be minor.

The primary structural differences that are observed by diffraction methods between carbonyl Hbs and Mbs should reflect the enhanced presence of the band I conformer at

~1938 cm^{-1} in most Mbs (1933 cm^{-1} in sperm whale) (Caughey et al., 1983) and would appear to correspond to a band I CO in Mb CO that is off normal by 120° (Kuriyan et al., 1986).

Conclusion

We have presented a variety of HbCO species that exhibit multiple CO IR conformers related to the steric constraints of the heme pocket. Distal interactions play a predominant role in determining the vibrational band frequency and half-band widths. Most HbCO's exhibit only one well-defined conformer near 1951 cm^{-1}, which corresponds to a tightly packed distal ligand binding site. Very specific changes in amino acid residues are required to alter this "typical wild-type" conformer structure. A minor structure (band IV) present in all carbonyl Hb and Mb spectra (i.e., irrespective of the major conformer) appears to involve an enlargement of the heme pocket. The protein conformer interconversion is faster than 10^4/s. Various protein motions (including side-chain rearrangements of both the distal E-7 His and E-11 Val residues and/or more concerted motions involving elements of secondary structure) are likely to be involved in the ligand binding site enlargement. Heme-bound CO vibrational spectra can be used to quantitatively analyze the dynamic nature of the heme pocket in relationship to structural, ligand binding, and stability properties.

Registry No. HbACO, 9072-24-6.

References

Alben, J. O., & Caughey, W. S. (1968) *Biochemistry 7*, 175.

Alben, J. O., Beece, D., Bowne, S. F., Doster, W., Eisenstein L., Frauenfelder, H., Good, D., McDonald, J. D., Marden, M. C., Moh, P. P., Reinisch, L., Reynolds, A. H., Shyamsunder, E., & Yue, K. T. (1982) *Proc. Natl. Acad. Sci. U.S.A. 79*, 3744.

Alberding, N., Chan, S. S., Eisenstein, L., Frauenfelder, H., Good, D., Gunsalus, I. C., Nordlund, T. M., Perutz, M. F., Reynolds, A. H., & Sorensen, L. B. (1978) *Biochemistry 17*, 43.

Andersson, L., Bengtsson, S., Hellman, U., Kallman, I., & Ranje, C. (1985) *Anim. Blood Groups Biochem. Genet. 16*, 41.

Antonini, E., & Brunori, M. (1971) in *Hemoglobin and Myoglobin in Their Reactions with Ligands* (Neuberger, A., Ed.) pp 1–427, North-Holland, New York.

Berzofsky, J. A., Peisach, J., & Alben, J. O. (1972) *J. Biol. Chem. 247*, 3774.

Brown, W. E., Sutcliffe, J. W., & Pulsinelli, P. D. (1983) *Biochemistry 22*, 2914.

Campbell, B. F., Magde, D., & Sharma, V. S. (1985) *J. Biol. Chem. 260*, 2752.

Carson, S. D., Constantinidis, I., Satterlee, J. D., & Ondrias, M. R. (1985) *J. Biol. Chem. 260*, 8741.

Case, D. A. & Karplus, M. (1979) *J. Mol. Biol. 132*, 343.

Caughey, W. S. (1970) *Ann. N. Y. Acad. Sci. 174*, 148.

Caughey, W. S. (1980) in *Methods for Determining Metal Ion Environments in Proteins: Structure and Function of Metalloproteins* (Darnall, D. W., & Wilkins, R. G., Eds.) p 95, Elsevier, North-Holland, New York.

Caughey, W. S., Houtchens, R. A., Lanir, A., Maxwell, J. C., & Charache, S. (1978) in *Biochemical and Clinical Aspects of Hemoglobin Abnormalities* (Caughey, W. S., Ed.) p 29, Academic Press, New York.

Caughey, W. S., Shimada, H., Choc, M. G., & Tucker, M. P. (1981) *Proc. Natl. Acad. Sci. U.S.A. 78*, 2903.

Caughey, W. S., Shimada, H., Tucker, M. P., Kawanishi, S., Yoshikawa, S., & Young, L. J. (1982) in *Oxygenases and Oxygen Metabolism* (Nozaki, M., Yamamoto, S., Ishimura, Y., Coon, M. J., Ernster, L., & Estabrook, R. W., Eds.) p 429, Academic Press, New York.

Caughey, W. S., Shimada, H., Hazzard, J. H., Houtchens, R. A., Potter, W. T., & Einarsdottir, O. (1983) *Fed. Proc., Fed. Am. Soc. Exp. Biol. 42*, 2000.

Chance, M. R., Campbell, B. F., Hoover, R., & Friedman, J. M. (1987) *J. Biol. Chem. 262*, 6959.

Choc, M. G., & Caughey, W. S. (1981) *J. Biol. Chem. 256*, 1831.

Deathrage, J. F., Loc, R. S., Anderson, C. M., & Moffat, K. (1976) *J. Mol. Biol. 104*, 687.

Dong, A., Messerschmidt, R. G., Reffner, J. A., & Caughey, W. S. (1988) *Biochem. Biophys. Res. Commun. 156*, 752.

Fermi, G., Perutz, M. F., Shaanan, B., & Fourme, R. (1984) *J. Mol. Biol. 175*, 159.

Fraser, R. D. B., & Suzuki, E. (1969) *Anal. Chem. 41*, 37.

Giacommetti, G. M., Brunori, M., Antonini, E., DiIorio, E. E., & Winterhalter, K. H. (1980) *J. Biol. Chem. 255*, 6160.

Gilman, J. G., & Brewer, G. J. (1978) *Biochem. J. 169*, 625.

Hegetschweiler, K., Saltman, P., Dalvit, C., & Wright, P. E. (1987) *Biochim. Biophys. Acta 912*, 384.

Heidner, E. J., Ladner, R. C., & Perutz, M. F. (1976) *J. Mol. Biol. 104*, 707.

Jelkman, W., & Bauer, C. (1976) *Anal. Biochem. 75*, 382.

Kawanishi, S., & Caughey, W. S. (1985) *J. Biol. Chem. 260*, 4622.

Kuriyan, J., Wilz, S., Karplus, M., & Petsko, G. A. (1986) *J. Mol. Biol. 192*, 133.

Liddington, R., Derewenda, Z., Dodson, G., & Harris, D. (1988) *Nature 331*, 725.

Makinen, M. W., Houtchens, R. A., & Caughey, W. S. (1979) *Proc. Natl. Acad. Sci. U.S.A. 76*, 6042.

Maxwell, J. C., & Caughey, W. S. (1978) *Methods Enzymol. 54*, 302.

McCoy, S., & Caughey, W. S. (1971) in *Probes of Structure and Function of Macromolecules and Membranes* (Chance, B., Yonetani, T., & Mildvan, A. S., Eds.) Vol. II, p 289, Academic Press, New York.

Moffat, K., Deatherage, J. F., & Seybert, D. W. (1979) *Science 206*, 1035.

Moh, P. P., Fiamingo, F. G., & Alben, J. O. (1987) *Biochemistry 26*, 6243.

Moon, R. B., & Richards, J. H. (1974) *Biochemistry 13*, 3437.

Moon, R. B., Dill, K., & Richards, J. H. (1977) *Biochemistry 16*, 221.

Nagai, K., Luisi, B., Shih, D., Miyazaki, G., Imai, K., Poyart, C., De Young, A., Kwiatkowsky, L., Noble, R. W., Lin, S.-H., & Yu, N.-T. (1987) *Nature 329*, 858.

Oelshegel, F. J., Jr., Brewer, G. J., Knutsen, C., Prasad, A. S., & Schoomaker, E. B. (1973) *Biochem. Biophys. Res. Commun. 53*, 560.

Onwubiko, H. A., Hazzard, J. H., Noble, R. W., & Caughey, W. S. (1982) *Biochem. Biophys. Res. Commun. 106*, 223.

Potter, W. T., Hazzard, J. H., Kawanishi, S., & Caughey, W. S. (1983) *Biochem. Biophys. Res. Commun. 116*, 719.

Potter, W. T., Houtchens, R. A., & Caughey, W. S. (1985) *J. Am. Chem. Soc. 107*, 3350.

Potter, W. T., Tucker, M. P., Houtchens, R. A., & Caughey, W. S. (1987) *Biochemistry 26*, 4699.

Ribarov, S. R., Benov, L. C., & Benchev, I. C. (1981) *Biochim. Biophys. Acta 664*, 153.

Riggs, A. (1981) *Methods Enzymol. 76*, 8.
Ringe, D., Petsko, G. A., Kerr, D. E., & Ortiz de Montellano, P. R. (1984) *Biochemistry 23*, 2.
Sampath, V., & Caughey, W. S. (1985) *J. Am. Chem. Soc. 107*, 4076.
Satterlee, J. D. (1983) *Inorg. Chim. Acta 79*, 170.
Satterlee, J. D., Teintze, M., & Richards, J. H. (1978) *Biochemistry 17*, 1456.
Sharma, V. S., & Ranney, H. M. (1982) *J. Mol. Biol. 158*, 551.
Sharma, V. S., Vedvick, T. S., Magde, D., Luth, R., Friedman, D., Schmidt, M. R., & Ranney, H. M. (1980) *J. Biol. Chem. 255*, 5879.
Shimada, H., & Caughey, W. S. (1982) *J. Biol. Chem. 257*, 11893.
Shimada, H., Dong, A., Ishimura, Y., & Caughey, W. S. (1989) *Biochem. Biophys. Res. Commun. 158*, 110.
Smith, M. L., Paul, J., Ohlson, P. I., & Paul, K. G. (1984) *Biochemistry 23*, 6776.
Stenzel, P., Brimhall, B., Jones, R. T., Black, J. A., McLachian, A., & Gibson, D. (1979) *J. Biol. Chem. 254*, 2071.
Tucker, P. W., Phillips, S. E. V., Perutz, M. F., Houtchens, R., & Caughey, W. S. (1978) *Proc. Natl. Acad. Sci. U.S.A. 75*, 1076.
Wallace, W. J., & Caughey, W. S. (1975) *J. Am. Chem. Soc. 107*, 4076.
Yoshikawa, S., O'Keeffe, D. H., & Caughey, W. S. (1985) *J. Biol. Chem. 260*, 3518.
Yu, N.-T., Kerr, E. A., Ward, B., & Chang, C. K. (1983) *Biochemistry 22*, 4534.

High Mobility Group Proteins 1 and 2 Function as General Class II Transcription Factors†

Jagmohan Singh*,‡ and Gordon H. Dixon

Department of Medical Biochemistry, Health Sciences Center, University of Calgary, 3330 Hospital Drive N.W., Calgary, Alberta T2N 4N1, Canada

Received February 7, 1990; Revised Manuscript Received March 27, 1990

ABSTRACT: High mobility group (HMG) proteins 1 and 2 are thought to be associated with chromatin enriched in active gene sequences, to stimulate endogenous transcription of class II and III genes using HMG-depleted nuclei, and to bind specific DNA sequences upstream of the coding regions of trout HMG-T and human β-globin genes. In testing the possibility that these proteins may act as general transcription factors, the run-off transcription of trout protamine, human β-globin, adenovirus 2 major late promoter, and herpes simplex virus (HSV) thymidine kinase genes was found to be inhibited by affinity-purified HMG-1 and -2 antibodies. The inhibition was partially relieved by exogenously added HMG-1 or -2. A complementation assay showed that the 0.15 M KCl flowthrough of HeLa nuclear extract fractionated by anion-exchange chromatography (DE-52) could be replaced by purified HMG-1 and/or -2 to complement transcription of the trout protamine gene by the 0.5 M KCl eluate fraction. Inhibition studies with heparin showed that HMG-1 and -2 were required for initiation of transcription. These results indicate an absolute requirement of HMG-1 and -2 for class II gene transcription. Western blotting and transcription reconstituted with purified factors show a copurification of HMG-1 and -2 with factor II B, described earlier by Reinberg and Roeder [(1987) *J. Biol. Chem. 262*, 3310–3321].

The structure, localization, and function of high mobility group proteins have been extensively studied since their discovery by E. W. Johns [reviewed in Johns (1982)]. Their presence in a variety of eukaryotic species (Mayes, 1982) suggests that they perform some important biological function(s). Moreover, the genetic inactivation of the gene for a yeast HMG-like protein (ACP-2) with sequence similarity to HMG-1/-2 has recently been shown to be lethal (Haggren & Kolodrubetz, 1988). Dixon and co-workers (Hutcheon et al., 1980; Levy et al., 1977a,b) and Weintraub and co-workers (Weintraub & Groudine, 1976; Weisbrod & Weintraub, 1980) showed that the smaller HMG's, namely, HMG-14 and -17 (molecular weight ≈10 000 each) and H6, their trout counterpart, were preferentially associated with transcriptionally active genes. Weintraub and co-workers showed that at the level of both intact chromatin and isolated nucleosomes of chicken reticulocytes, the DNase 1 sensitivity of the active globin gene was due to association with HMG-14 and -17 (Mardian et al., 1980; Weisbrod et al., 1980). How HMG-14 and -17, which appear to bind to DNA at the entry and exit to the nucleosome (Mardian et al., 1980), could recognize potentially active nucleosomes as opposed to the bulk, inactive nucleosomes was not clear. Recently, antibody probing has shown that HMG-17 is localized on chromatin of transcribed genes only downstream from the starting point of transcription (Dorbic & Wittig, 1987).

In contrast with the studies on HMG-14 and -17 and H6, no clear function has been established for the larger HMG's, HMG-1 and -2 (molecular weight ~25 000–30 000). They have been shown to be associated with nucleosomes of active genes (Jackson et al., 1979; Vidali et al., 1977), and HMG-T, their trout counterpart, appeared, by antibody binding, to be

† This work was supported by grants from the Alberta Heritage Foundation for Medical Research and the Medical Research Council of Canada.
* Author to whom correspondence should be addressed.
‡ Present address: NCI–Frederick Cancer Research Facility, BRI–Basic Research Program, P.O. Box B, Frederick, MD 21701.

0006-2960/90/0429-6295$02.50/0 © 1990 American Chemical Society